Regulatory DNA keyholes enable specific and persistent multi-gene expression programs in primary T cells without genome modification

Matthew S. Wilken[1,†], Christie Ciarlo[1,†], Jocelynn Pearl[1,†,††], Jordan Bloom[1], Elaine Schanzer[1], Hanna Liao[1], Scott E. Boyken[2,3,††], Benjamin Van Biber[1], Konstantin Queitsch[1], Gregory Heberlein[1], Alexander Federation[1], Reyes Acosta[1], Shinny Vong[1], Ericka Otterman[1], Douglass Dunn[1], Hao Wang[1], Pavel Zrazhevskey[1], Vivek Nandakumar[1], Daniel Bates[1], Richard Sandstrom[1], Zibo Chen[2,3,†††], Fyodor D. Urnov[1], David Baker[2,3,4], Alister Funnell[1], Shon Green[1], and John A. Stamatoyannopoulos[1,5,*].

Affiliations:

[1]*Altius Institute for Biomedical Sciences (Nonprofit), Seattle, WA, USA.*
[2] *Department of Biochemistry, University of Washington, Seattle, WA, USA.*
[3] *Institute for Protein Design, University of Washington, Seattle, WA, USA.*
[4] *Howard Hughes Medical Institute, University of Washington, Seattle, WA, USA.*
[5] *Departments of Genome Sciences and Medicine, University of Washington, Seattle, WA, USA.*
[†] *Equal contribution*
[††] *Current address: Lyell Immunopharma, Inc., Seattle, WA 98109, USA.*
[†††] *Current address: Dept. of Biology, California Institute of Technology, Pasadena, CA, USA.*

[*]Correspondence: jstam@altius.org or jstam@uw.edu.

Abstract

Non-invasive epigenome editing is a promising strategy for engineering gene expression programs, yet potency, specificity, and persistence remain challenging. Here we show that effective epigenome editing is gated at single-base precision via 'keyhole' sites in endogenous regulatory DNA. Synthetic repressors targeting promoter keyholes can ablate gene expression in up to 99% of primary cells with single-gene specificity and can seamlessly repress multiple genes in combination. Transient exposure of primary T cells to keyhole repressors confers mitotically heritable silencing that persists to the limit of primary cultures *in vitro* and for at least 4 weeks *in vivo*, enabling manufacturing of cell products with enhanced therapeutic efficacy. DNA recognition and effector domains can be encoded as separate proteins that reassemble at keyhole sites and function with the same efficiency as single chain effectors, enabling gated control and rapid screening for novel functional domains that modulate endogenous gene expression patterns. Our results provide a powerful and exponentially flexible system for programming gene expression and therapeutic cell products.

Main

Transcription factors (TFs) convert information encoded in regulatory DNA regions such as promoters and enhancers into gene expression and cell state outcomes. TFs are modular proteins that combine a DNA recognition domain with one or more domains that confer specific functions via interplay with other chromatin proteins[1, 2]. A key aspect of TF function derives from an ability to engage with double-stranded DNA and interact with native regulatory architectures assembled on the same template; notably, this property is not maintained in RNA-guided protein-DNA recognition, which involves extensive unwinding and disruption of the native DNA template[3]. The advent of synthetic DNA binding domains comprising linear combinations of zinc finger[4, 5] or transcriptional activator-like (TAL)[6, 7] DNA base recognition modules enables, in principle, the ability to program gene expression via selective targeting of covalently-linked functional activities to regulatory regions.

Systematic application of synthetic transcription factors for both basic and clinical research will require effectors that (i) can be targeted to precise genomic positions, (ii) are highly potent, and (iii) show single-gene-specific activity. The ability to program gene expression reliably without the potentially genotoxic sequelae of nucleases holds particular promise in therapeutic cell engineering [8-14]. However, little is currently known concerning the precise mode(s) through which TF functional domains interact with native chromatin proteins to trigger changes in the expression of a specific gene.

Despite decades of work on repressive domains such as the Kruppel-associated box (KRAB) [17, 22], it remains unclear what factors contribute to its activity in the context of a given promoter region. In general, observed potencies have been highly variable, and complete repression has been elusive. Additionally, the impact of different types of functional domains on gene repression has been difficult to assess due to widely varying (or unreported) efficiencies of DNA targeting. Achieving high specificity has been extremely challenging, with the result that potent single gene-specific repression in primary cells has not been achieved.

While the potential for establishing mitotically heritable gene expression states appears to exist for a subset of genes harboring CpG islands within their promoter regions[15-17], existing studies have not identified broadly-applicable tools or rules for conferring heritable gene expression programs on endogenous, dynamically regulated genes in primary cells. Prior attempts to engineer durable transcriptional repression have chiefly employed reporter constructs randomly integrated into transformed cell lines[16-19] vs. targeting of endogenous genes. As such, while the potential for mitotically heritable repression exists, its observation has been widely variable, and it has not been possible to disentangle contributions of binding, genomic position, and choice of functional domain.

Here we report that the potency and specificity of epigenetic transcriptional repression are linked through promoter keyhole sites, the targeting of which triggers near-complete repression with single-gene accuracy. Potent repression, in turn, enables durable programming via reliable induction of mitotically heritable expression programs, offering new potential for engineered cell therapies.

Results

Here we report the development of highly potent, specific, and mutliplexable synthetic repressors that can be deployed in primary human T cells to durably repress therapeutically relevant endogenous genes. Additionally, we dramatically broaden the application of synthetic repressors using a modular split system wherein DNA recognition and effector domains are encoded on separate polypeptides.

For DNA recognition, we used the *Xanthomonas* TAL effector repeats [6, 7], which enable modular synthesis of DNA binding domains (DBDs) capable of targeting ~95% of the human genome sequence[12, 20-22]. Synthetic TAL DBDs (T-DBDs) can be appended at either their C- or N-termini with effector domains conferring function in mammalian cells – for example the KRAB repressor domain[15, 23]. In both native and artificial TFs, KRAB domains recruit the KAP1 co-repressor and, in turn, endogenous enzymatic complexes that methylate histones and DNA and trigger focal heterochromatin formation[23-28].

Nucleotide-precise gating of epigenetic repression

We focused initially on two major immune checkpoint genes: *HAVCR2* (TIM3) and *LAG3,* both of which encode cell surface molecules. Using a combination of DNase-seq and RNA-seq to map empirically the zone of transcription initiation [29] for each gene in primary T cells, we designed a series of densely spaced synthetic T-DBD-KRAB repressors targeting these regions (Fig. 1A,B). To quantify efficacy, we electroporated repressor mRNA into primary T cells and measured the proportion of TIM3- or LAG3-positive cells 48 hours post electroporation. *A priori,* we expected that repressors targeting the same small region would be nearly equivalent in function. Instead, for both genes we found that most synthetic repressors exhibited little to no function, while a small number exhibited highly effective gene repression. Highly potent repressors were limited to specific promoter positions; four non-contiguous TIM3 repressors exhibited strong repression, with one (TM18) producing near-complete silencing, as did four *LAG3* repressors with partially overlapping recognition sites distributed over ~15bp (Fig. 1C-E). Repression was accompanied by loss of H3K4me3 and gain of H3K9me3 as expected for KRAB-induced silencing (Fig. S1). For both genes, targeting only a few nucleotides 5' or 3' did not evince significant repression. Similar findings were evident when we repeated the above for another immune checkpoint gene, *PDCD1*(PD-1) (not shown). As such, the ability of synthetic DBD-KRABs to trigger repressor activity appears to be confined to highly specific 'keyhole' sites within gene promoters.

We speculated that the keyhole phenomenon might result from tight positional (and hence rotational) constraints on the presentation of the KRAB domain. To test this, we devised a strategy for migrating the KRAB domain at 1bp intervals along both strands of a 115 bp region overlapping the keyhole site within the LAG3 promoter by means of synthetic repressors with incrementally extended DNA binding domains (Fig. 1F, S2A). This revealed discrete locations where migrating the KRAB domain even 1 bp 3' or 5' was sufficient to trigger strong repression from otherwise identical T-DBD-KRAB molecules (Fig. 1G, S2B,C). These results indicate that the epigenetic silencing cascade initiated by KRAB is precisely triggered at single nucleotide resolution by its linear (and hence rotational) positioning within promoter chromatin.

Multiplex repression without loss of potency or specificity

Delivery of potent TIM3 and LAG3 repressors (TM18 and LG09, respectively) both separately and simultaneously produced linearly additive results (Fig. 1E), indicating that synthetic repressors could be combined with no loss of potency. To quantify the specificity of repression – a key parameter for functional studies and potential clinical application – we measured global differential RNA transcription by total RNA-seq in primary T-cells 48h following electroporation of synthetic keyhole repressors of *HAVCR2* (TIM3), *LAG3*, and *PDCD1* (PD-1), applied individually (Fig. 2A-C, genome browser views, left) or simultaneously (Fig. 2D). Individual repressors ablated RNA expression of their target genes with near complete specificity (Fig. 2A-C, volcano plots, right). Of note, the *LAG3* repressor resulted in down-regulation of the closely-positioned gene *PTMS* located ~1kb upstream (Fig. 2B), consistent with a +/- ~2kb H3K9me3 'halo' produced by KRAB-triggered silencing (Fig. S1). Notably, while *LAG3* was completely repressed, *PTMS* was only partially repressed (35% of control) (Fig. 2B).

Simultaneous delivery of all three repressors produced additive effects with no loss of potency or specificity (Fig. 2D). We also observed both additivity and dose-dependence at the level of a single gene targeted by multiple synthetic repressors directed to different keyhole sites within the same promoter (Fig. S3). Synthetic repressors targeting keyhole sites thus exhibit both high potency and remarkable specificity and can be combined additively to produce T cell products with defined multi-gene expression patterns.

Epigenetic persistence of gene repression programs

We next studied the duration of the repressive effect as a function of synthetic repressor persistence. Repressor mRNA and protein are rapidly degraded, with protein returning to background levels by 48h post mRNA electroporation (Fig. S4). Following CD3/CD28 stimulation, primary T cells begin cycling with a doubling time of approximately 36 hrs. As such, effects on gene expression persisting beyond 72 hours reflect mitotically heritable states. In mock transfected cells, TIM3 expression peaks at ~8 days post stimulation before beginning a gradual decline to steady state levels of ~40% TIM3+ cells (Fig. 3A, open circles). By contrast, cells receiving the TM18 repressor show near complete repression of TIM3 up to day 5 post electroporation (day 7 post stimulation), and declining persistence of repression for another ~20 days, nearing the practical limit of T cell culture (Fig. 3A, solid black circles, red trace). The synthetic repressor targeting PD-1 provided nearly full repressive effect for two weeks in culture (Fig. 3B).

To test for persistence of mitotically heritable repression in a longer duration, physiologically meaningful *in vivo* milieu, we applied a synthetic PD-1 repressor (PD02) to human T cells expressing an anti-CD19 chimeric antigen receptor (CAR) and infused these cells after 1 week in culture into female NOD/SCID gamma mice [30] that had been implanted five days prior with $5x10^5$ human B-cell acute lymphoblastic leukemia (ALL) cells expressing CD19 (NALM-6 cells [31]), at a dose expected to rapidly clear the leukemia cells. In this physiologically stimulated milieu, serial peripheral blood measurements revealed persistence of PD-1 repression in infused T cells for 4 weeks post infusion, and thus 5 weeks post repressor transfection (Fig. 3C,D). As such, a transient pulse of a synthetic keyhole repressor is capable of establishing a mitotically-

heritable expression state at its target gene that persists within a substantial fraction of cells for an extended interval in a challenging *in vivo* setting.

Therapeutic enhancement of CAR-T cells

We next asked whether keyhole repressors of immune checkpoint genes, either alone or in combination, could potentiate CAR-T cell efficacy *in vivo*. To test this, we engineered human anti-CD19 CAR-T cell products treated (separately) with keyhole repressors targeting PD-1, TIM3, and LAG3, and a multiplex dose of all three repressors simultaneously. The former achieved 98-99% repression of individual target genes, and the latter yielded a cell product with >97% of cells lacking PD-1, TIM-3, or LAG-3 (Fig. 3E). We infused NSG mice (separately) with $2.5x10^5$ CAR-T cells from each of these engineered cell products (plus non-engineered cell and CAR-T only controls) 6 days post NALM-6 tumor implantation (5 mice per arm). All mice receiving CAR-T cells had no detectable tumor by 8 days post-infusion (14 days post tumor implantation) (Fig. 3E-G), representing initial clearing of tumor by CAR-T. We then re-challenged the mice with additional tumor cells at 21 days post-infusion (27 days post initial tumor implantation), a time when very few human CD3+ cells could be detected in peripheral blood (data not shown). Mice that received multiplex repressed (PD-1/LAG3/TIM3-negative) CAR-T cells showed superior tumor control, with no relapses observed at 47 days post initial tumor infusion (20 days post second tumor challenge) versus relapses in CAR-T-only or single checkpoint gene repressed cells. These results suggest that combining CARs with potent and durable epigenetic silencing of multiple immune checkpoint genes via keyhole repressors has the potential to increase the efficacy of therapeutic cell products.

Split encoding of DNA binding and functional domains

Having demonstrated high performance of synthetic transcription factor repressors for programming single or multiplex gene expression *in vitro* and *in vivo*, we next sought to develop an approach for generating complex synthetic factors capable of generating diverse cellular programs. Split encoding of DNA targeting and functional activities on separate molecules, as exemplified in RNA-guided systems such as Cas/CRISPR, offers substantial potential for flexibility and scale. We reasoned that if synthetic repressors could be decomposed into separately delivered T-DBDs and repressor domains that assembled *in situ*, it would be possible to screen large numbers of functional alternatives to KRAB by delivering them to the same keyhole site. It would also open new avenues for implementing complex combinatorial cell engineering programs.

Orthogonal protein heterodimer pairs [32] offer an attractive system for ordered protein-protein pairing. However, the ability of such pairs to function in the complex environment of human cells is unknown. We first tested whether T-DBD and KRAB domains could be split and efficiently assembled following electroporation as separate molecules. We designed modified synthetic repressors that incorporated one half of an orthogonal protein heterodimer pair (*1* and *1'*) (see Methods) after the C-terminal residue of the PD-1 synthetic repressor T-DBD. On a separately encoded molecule, we engineered its cognate half upstream of the N-terminal residue of KRAB. Introduction of either the separately encoded T-DBD/heterodimer or heterodimer/KRAB proteins alone showed no effects on PD-1 gene expression (Fig. 4A, left). By contrast, parallel electroporation of separate mRNAs encoding each molecule produced potent repression nearly indistinguishable from that of the same T-DBD/KRAB synthetic

repressor encoded by a single chain polypeptide (Fig. 4A, right and Fig. S5). As such, an obligate heterodimer pair can enable the DNA binding and functional domains of synthetic transcription factors to be split and separately delivered in a flexible, and potentially highly scalable, manner.

Alternative domains modulate persistence of repression

To enrich further the functional repertoire of synthetic split TFs (SSTFs), we next explored the impacts on both potency and target expression kinetics of a wide range of candidate repressor domains extracted from native human TFs by delivering them to the keyhole site in the TIM3 promoter targeted by the DBD of TM18 (Fig. 4B,C). We co-delivered TM18-DBD-*1* mRNA into primary human T-cells together with mRNA encoding each (separately) of the 77 candidate repressive domains shown in Fig. 4C fused to the *1'* heterodimer (Fig. 4D), and assayed TIM3 expression by flow cytometry over a 26 day interval. We identified numerous highly active repressive domains that differed chiefly in their temporal kinetics of repression (Fig. 4E,F). Some SSTFs displayed an immediate sharp decline in repression at 5 days and complete loss by 2 weeks (Fig. 4F). In contrast, different KRAB domain homologs from human zinc finger proteins exhibited a relatively slow kinetic profile of de-repression that extended to at least 26 days (Fig. 4E). The spatial presentation of functional domains, whether fused to the heterodimer at the C- or N-terminus, altered the repressive efficacy of at least one domain (MBD2), but not others (KRAB, CTBP1, and MECP2) (Fig. S6). Notably, we observed only modest repressive activity for DNA methyltransferase domains [16, 33] when combined with the DNA binding domain of TM18, PD02, or LG09 (not shown).

The above results thus show that SSTFs can be used to deliver different functional activities to the same keyhole site (or any other targeted site) at scale and indicate that different classes of repressive domains encoded within native TFs may confer different functions that are reflected chiefly in the kinetics of repression.

Discussion

In summary, we have shown that synthetic TFs combining TAL-DBDs with native repressor domains from human TFs are capable of producing near-complete gene silencing in primary T cells with extremely high specificity, in contrast to prior efforts [16, 17, 34]. Repression is triggered at single nucleotide resolution, indicating a critical dependence on the spacing and rotational presentation of functional domains within promoters, which in turn relies on precise interactions with the native double-stranded DNA template. The remarkable potency, specificity, and additivity of keyhole repressors enable engineering of highly pure and potentially safer T cell products. The epigenetic durability of repression (>4 weeks *in vivo*) parallels the clinical effectiveness windows of recently described engineered cell therapies targeting lymphoid malignancies [35], opening the door for creation of epigenetically engineered therapeutic cell products with defined kinetics or natural 'off switches'. As proof of concept, multiplex repression of the immune checkpoint genes PD-1, LAG3, and TIM3 in anti CD19 CAR-T cells resulted in enhanced efficacy compared with any individual repressor in a tumor re-challenge experiment, suggesting that this combination confers enhanced persistence and/or resistance to exhaustion.

The ability to encode DNA targeting and functional activities on separate molecules with full retention of function that is conferred by obligate heterodimers offers unprecedented potential to create novel regulatory molecules that can be combined to

program complex cell states. The availability of multiple orthogonal heterodimer pairs expands the effector engineering space exponentially, enabling *in vivo* assembly of polyfunctional molecules (Fig. S7A-D), and encoding of logic gates, among other applications. It should also be straightforward to incorporate split encoding of native double-strand DNA recognition and diverse functional activities into vector platforms (Fig. S7E) to enable highly complex large-scale genetic and epigenetic screening applications.

References and Notes:

1. Lambert, S.A. et al. The Human Transcription Factors. *Cell* **172**, 650-665 (2018).
2. Brent, R. & Ptashne, M. A eukaryotic transcriptional activator bearing the DNA specificity of a prokaryotic repressor. *Cell* **43**, 729-736 (1985).
3. Nishimasu, H. et al. Crystal structure of Cas9 in complex with guide RNA and target DNA. *Cell* **156**, 935-949 (2014).
4. Choo, Y., Sanchez-Garcia, I. & Klug, A. In vivo repression by a site-specific DNA-binding protein designed against an oncogenic sequence. *Nature* **372**, 642-645 (1994).
5. Beerli, R.R., Segal, D.J., Dreier, B. & Barbas, C.F., 3rd Toward controlling gene expression at will: specific regulation of the erbB-2/HER-2 promoter by using polydactyl zinc finger proteins constructed from modular building blocks. *Proc Natl Acad Sci U S A* **95**, 14628-14633 (1998).
6. Boch, J. et al. Breaking the code of DNA binding specificity of TAL-type III effectors. *Science* **326**, 1509-1512 (2009).
7. Moscou, M.J. & Bogdanove, A.J. A simple cipher governs DNA recognition by TAL effectors. *Science* **326**, 1501 (2009).
8. Kosicki, M., Tomberg, K. & Bradley, A. Repair of double-strand breaks induced by CRISPR-Cas9 leads to large deletions and complex rearrangements. *Nat Biotechnol* **36**, 765-771 (2018).
9. Qi, L.S. et al. Repurposing CRISPR as an RNA-guided platform for sequence-specific control of gene expression. *Cell* **152**, 1173-1183 (2013).
10. Gilbert, L.A. et al. CRISPR-mediated modular RNA-guided regulation of transcription in eukaryotes. *Cell* **154**, 442-451 (2013).
11. Zhang, Z., Wu, E., Qian, Z. & Wu, W.S. A multicolor panel of TALE-KRAB based transcriptional repressor vectors enabling knockdown of multiple gene targets. *Sci Rep* **4**, 7338 (2014).
12. Maeder, M.L. et al. Targeted DNA demethylation and activation of endogenous genes using programmable TALE-TET1 fusion proteins. *Nat Biotechnol* **31**, 1137-1142 (2013).
13. Snowden, A.W. et al. Repression of vascular endothelial growth factor A in glioblastoma cells using engineered zinc finger transcription factors. *Cancer Res* **63**, 8968-8976 (2003).
14. Yeo, N.C. et al. An enhanced CRISPR repressor for targeted mammalian gene regulation. *Nat Methods* **15**, 611-616 (2018).
15. Mlambo, T. et al. Designer epigenome modifiers enable robust and sustained gene silencing in clinically relevant human cells. *Nucleic Acids Research* **46**, 4456-4468 (2018).

16. Amabile, A. et al. Inheritable Silencing of Endogenous Genes by Hit-and-Run Targeted Epigenetic Editing. *Cell* **167**, 219-232 e214 (2016).

17. Bintu, L. et al. Dynamics of epigenetic regulation at the single-cell level. *Science* **351**, 720-724 (2016).

18. O'Geen, H. et al. dCas9-based epigenome editing suggests acquisition of histone methylation is not sufficient for target gene repression. *Nucleic Acids Res* **45**, 9901-9916 (2017).

19. Fredericks, W.J., Ayyanathan, K., Herlyn, M., Friedman, J.R. & Rauscher, F.J., 3rd An engineered PAX3-KRAB transcriptional repressor inhibits the malignant phenotype of alveolar rhabdomyosarcoma cells harboring the endogenous PAX3-FKHR oncogene. *Mol Cell Biol* **20**, 5019-5031 (2000).

20. Cuculis, L., Abil, Z., Zhao, H. & Schroeder, C.M. Direct observation of TALE protein dynamics reveals a two-state search mechanism. *Nat Commun* **6**, 7277 (2015).

21. Mendenhall, E.M. et al. Locus-specific editing of histone modifications at endogenous enhancers. *Nature Biotechnology* **31**, 1133-1136 (2013).

22. Lo, C.L., Choudhury, S.R., Irudayaraj, J. & Zhou, F.C. Epigenetic Editing of Ascl1 Gene in Neural Stem Cells by Optogenetics. *Sci Rep* **7**, 42047 (2017).

23. Margolin, J.F. et al. Kruppel-associated boxes are potent transcriptional repression domains. *Proc Natl Acad Sci U S A* **91**, 4509-4513 (1994).

24. Groner, A.C. et al. The Kruppel-associated box repressor domain can induce reversible heterochromatization of a mouse locus in vivo. *J Biol Chem* **287**, 25361-25369 (2012).

25. Friedman, J.R. et al. KAP-1, a novel corepressor for the highly conserved KRAB repression domain. *Genes Dev* **10**, 2067-2078 (1996).

26. Bellefroid, E.J., Poncelet, D.A., Lecocq, P.J., Revelant, O. & Martial, J.A. The evolutionarily conserved Kruppel-associated box domain defines a subfamily of eukaryotic multifingered proteins. *Proc Natl Acad Sci U S A* **88**, 3608-3612 (1991).

27. Nawrath, M., Pavlovic, J. & Moelling, K. Inhibition of human hematopoietic tumor formation by targeting a repressor Myb-KRAB to DNA. *Cancer Gene Ther* **7**, 963-972 (2000).

28. Vissing, H., Meyer, W.K., Aagaard, L., Tommerup, N. & Thiesen, H.J. Repression of transcriptional activity by heterologous KRAB domains present in zinc finger proteins. *FEBS Lett* **369**, 153-157 (1995).

29. Neph, S. et al. An expansive human regulatory lexicon encoded in transcription factor footprints. *Nature* **489**, 83-90 (2012).

30. Shultz, L.D. et al. Human lymphoid and myeloid cell development in NOD/LtSz-scid IL2R gamma null mice engrafted with mobilized human hemopoietic stem cells. *J Immunol* **174**, 6477-6489 (2005).

31. Liu, X. et al. Improved anti-leukemia activities of adoptively transferred T cells expressing bispecific T-cell engager in mice. *Blood Cancer J* **6**, e430 (2016).

32. Chen, Z. et al. Programmable design of orthogonal protein heterodimers. *Nature* **565**, 106-111 (2019).

33. O'Geen, H. et al. Ezh2-dCas9 and KRAB-dCas9 enable engineering of epigenetic memory in a context-dependent manner. *Epigenetics Chromatin* **12**, 26 (2019).

34. Mlambo, T. et al. Designer epigenome modifiers enable robust and sustained gene silencing in clinically relevant human cells. *Nucleic Acids Res* **46**, 4456-4468 (2018).

35. Jain, T. et al. Utilization of Chimeric Antigen Receptor (CAR) T Cell Therapy in Clinical Practice for Relapsed/Refractory Aggressive B cell non-Hodgkin Lymphoma: An Expert Panel Opinion from the American Society for Transplantation and Cellular Therapy. *Biol Blood Marrow Transplant* (2019).

Author contributions: M.S.W., C.C., J.P., A.F., F.D.U., S.G. and J.A.S. designed the research. M.S.W., C.C., J.P., E.S., J.B., H.L., B.V.B., K.Q, G.H, A.F., R.A., S.V., E.O., and A.F. performed cell engineering experiments. Z.C., S.B., and D.B. designed obligate orthogonal heterodimer pairs. D.D., H.W., and D.B. performed RNA-seq and CUT&RUN experiments. P.Z. and V.N. performed imaging experiments. M.S.W., C.C., J.P., J.B., R.S., P.V., and V.N. analyzed data. M.S.W., C.C., S.G., and J.A.S. wrote the manuscript with input from other co-authors.

Competing interests: M.S.W., C.C., S.G, A.F., F.D.U., and J.AS. are listed as inventors on patent applications related to the subject matter of the paper; D.B., Z.C., and S.E.B. are listed as inventors on patent applications related to obligate heterodimers; J.P. and S.E.B. are employees of Lyell Immunopharma, a for-profit biotechnology company. D.B. is a scientific advisor to Lyell Immunopharma.

Data and materials availability: All RNA-seq and imaging data, software code used for analysis, protein sequences, protocols, and materials used in the experiments and data analysis will be made freely available.
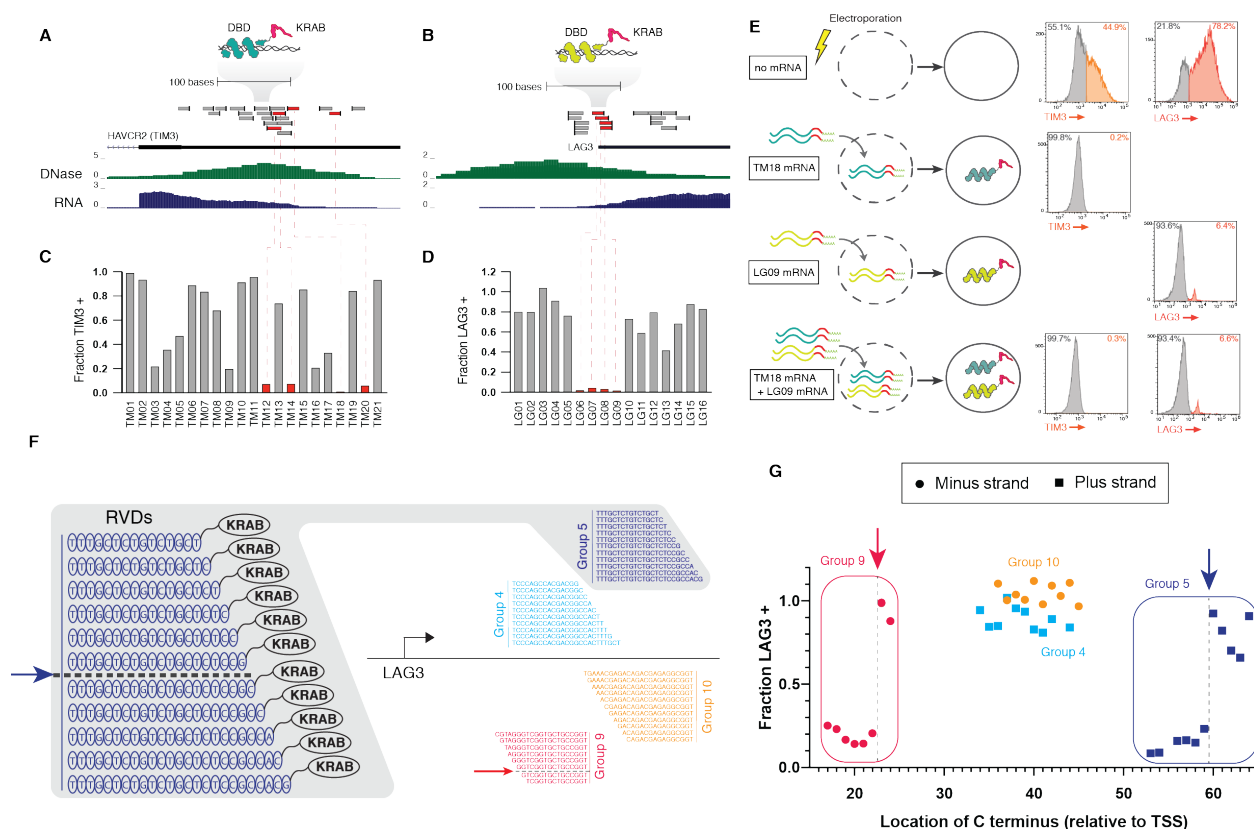
Fig. 1

Fig. 1. Potent silencing of gene expression in primary human T-cells triggered via nucleotide-precise placement of epigenetic repressor domains at keyhole sites. (a,b) Selection of repressors at the HAVCR2 (TIM3) and LAG3 promoters. Top: DNA binding domains (grey boxes) are shown to scale; tick marks indicate position of C-terminal KRAB domain. Red indicates 'keyhole' sites: DBD-KRABs with >90% repression. Bottom: DNase-seq and RNA-seq normalized tag density. (c,d) Fraction of TIM3+ or LAG3+ cells (normalized to mock transfection) as quantified by flow cytometry 48 hours after electroporation of repressor mRNA into activated CD3+ human T-cells. (e) Left, activated T-cells were electroporated with no RNA, or mRNAs encoding TM18, LG09, or both TM18 and LG09. Right, TIM3 and LAG3 surface protein expression quantified by flow cytometry at 48 hours post-transfection (plots representative of three independent experiments). (Note: Residual LAG3+ peak in repressor-treated cells results from bead autofluorescence of bead-cell complexes). (f) T-DBDs targeting seed sequences in the LAG3 promoter were sequentially extended by one repeat unit to produce groups of T-DBD-KRABs with different positioning of the C-terminal KRAB (see example group). (g) Fraction LAG3+ cells at 2 days post-transfection as measured by flow cytometry, normalized to no RNA controls. X-axis indicates the location of the KRAB domain relative to the LAG3 TSS. Groups 5 and 9 are highlighted to demonstrate loss/gain of repression activity when the KRAB domain was moved by one nucleotide.
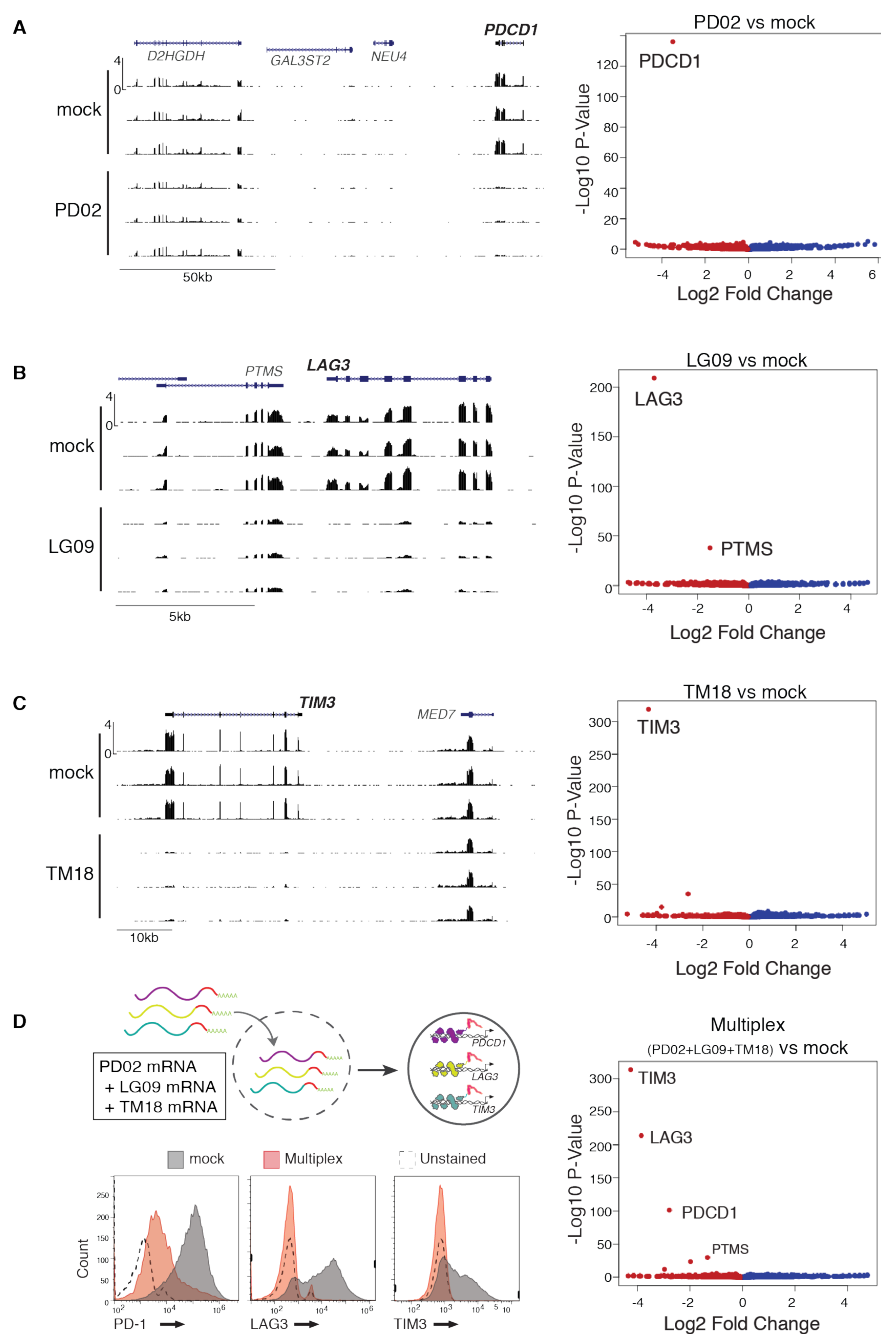
Fig. 2

Fig. 2. Multiplexing keyhole repressors does not affect individual potency or specificity (a) Left: RNA-seq tag density (scale bar in upper left) in PDCD1 locus following blank electroporation (top tracks, three independent replicates), and delivery of synthetic repressor PD02 targeting PDCD1 (bottom tracks, three independent replicates). Right: Volcano plot showing differential gene expression (RNA-seq q-value, vertical axis) following PD02 repressor delivery. (b) Results for LAG3 synthetic repressor, as for (a). (c) Results for TIM3 repressor, as for (a, b). Note that in addition to complete repression of LAG3, the PTMS gene

located 1.2kb upstream is partly repressed. (d) Left, co-delivery of PD02, LG09, and TM18 results in repression of target genes similar to individually delivered repressors. Right, volcano plot of differential gene expression (RNA-seq) q-values for co-delivered repressors consistent with linearly additive (and independent) contribution of each repressor.
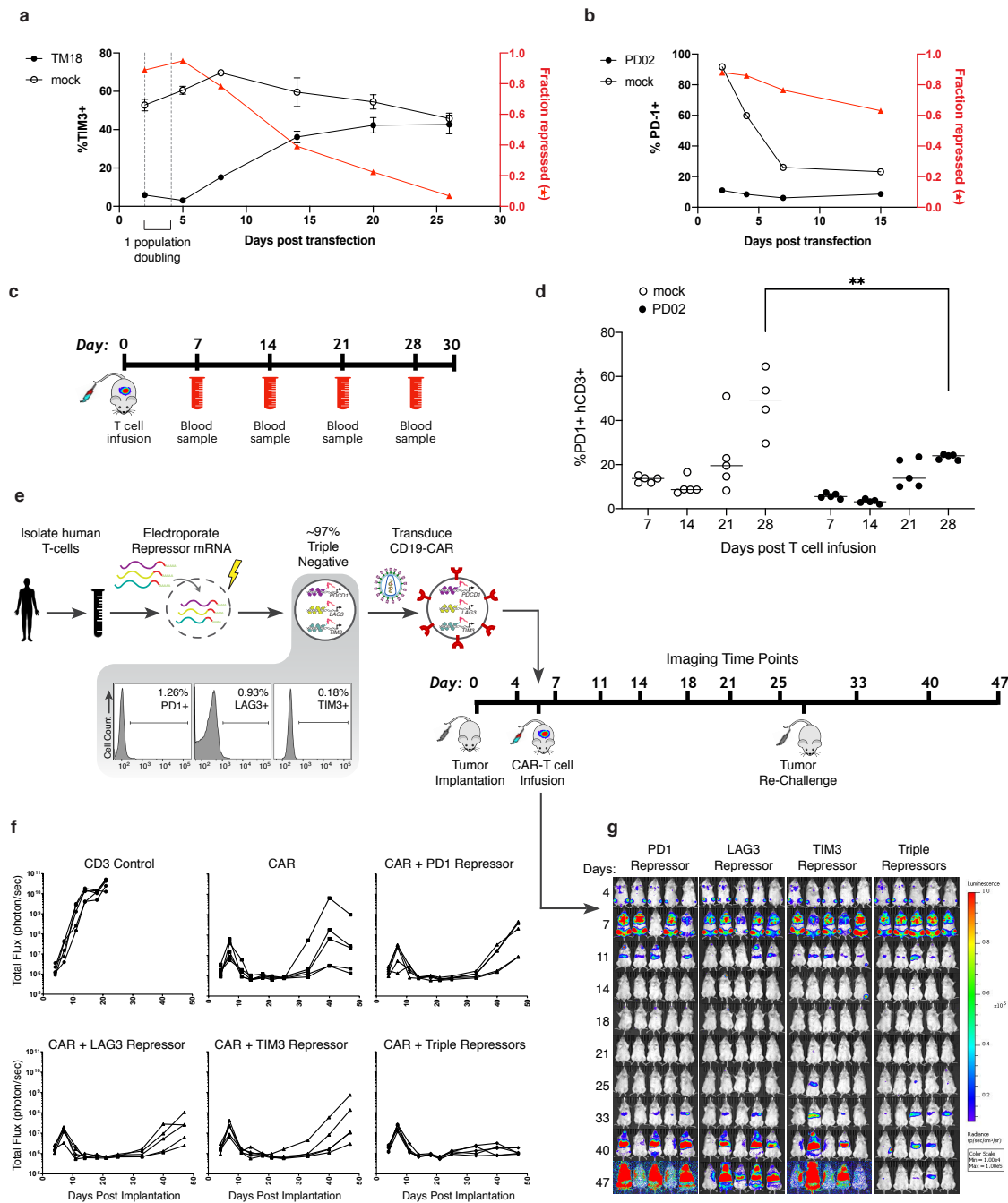
Fig. 3. Repression is durable for a therapeutically-relevant window in engineered primary T cells.   (a) Kinetics of TIM3 repression by synthetic repressor TM18. Primary T cells were electroporated with either no RNA or TM18 at day 0, and TIM3 expression was determined by cell surface antibody staining and flow cytometry for 26 days. Cells with greater fluorescence intensity than unstained control were considered TIM3+. Percent TIM3+ cells is indicated by dark colored lines and left y-axis. Fraction of cells with TIM3 repressed (%TIM3 negative cells in TM18-treated cells relative to no RNA control) is indicated by the right y-axis and red line.

Bars indicate standard deviation of two electroporations in the same experiment. Repression was maintained through a time period equivalent to one population doubling. Population doubling time was calculated assuming a constant proliferation rate and cell counts at days 2 and 5. (b) Kinetics of PD-1 repression by synthetic repressor PD02 as in (a). PD1 expression was determined over the course of 15 days post-electroporation. (c,d) PD-1 repression by PD02 is maintained for 28 days *in vivo* in CAR-T cells. Anti-CD19 CAR-T cells were transfected with either no RNA or PD02 and transplanted into mice bearing NALM-6 human B cell leukemia xenograft tumors. Mouse blood was sampled periodically for 28 days following CAR-T cell infusion, and percent of human CD3+ cells expressing PD1 was determined by cell surface antibody staining and flow cytometry. ** $P < 0.0066$ for day 28 samples. (e,f,g) Multiplexed repression of PD-1, LAG3, and TIM3 confers a therapeutic benefit over single immune checkpoint repression in a tumor rechallenge model *in vivo*. NSG mice were implanted with CD19-expressing NALM-6 B-ALL tumors and treated with anti CD19 CAR-T cells programmed with synthetic repressors (e). Tumor burden was measured as total bioluminescence at the indicated timepoints (e). Total flux spider plots and mouse images show relapse in all treatment groups after rechallenge with tumor cells, with the exception of the CAR-T cells programmed with multiplexed repressors (f,g).
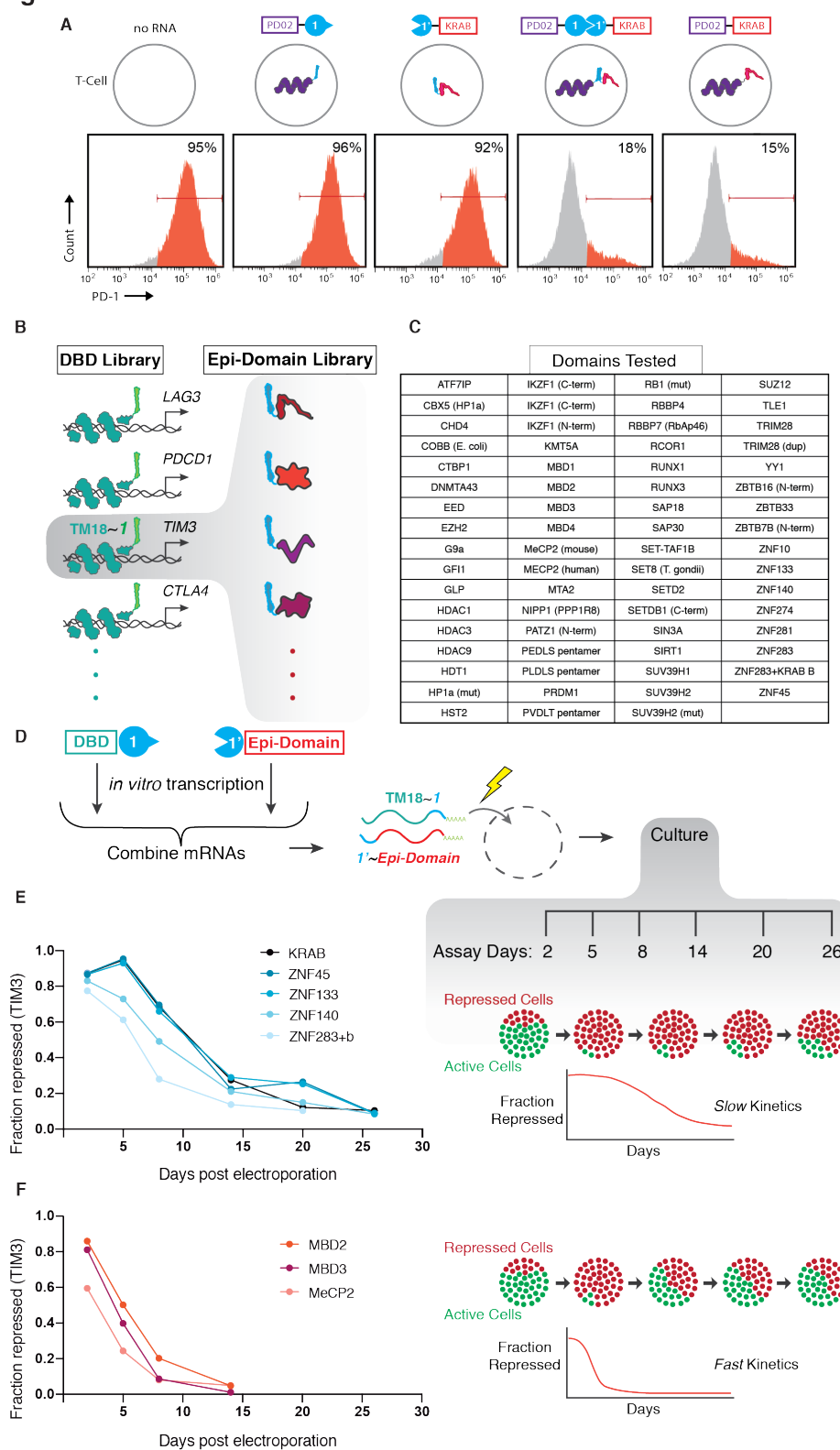
Fig. 4. Split system using obligate heterodimers enables potent repression and large-scale analysis of functional domains. (a) Activated primary human T cells were electroporated with

no RNA or components of synthetic repressor PD02 targeting PD-1. Cells were electroporated with: no RNA, DNA binding domain fused to heterodimer *1* (PD02-*1*) alone, KRAB domain fused to heterodimer *1'* (*1'*-KRAB) alone, both DNA binding domain and KRAB fused to respective heterodimers (equimolar amounts of separate molecules, combined in same electroporation), or DNA binding domain fused to KRAB (PD02-KRAB). Electroporated components indicated as cartoons above respective FACS plots. PD-1 expression was determined by cell surface antibody staining and flow cytometry 48 hours after electroporation. (b) Conceptual diagram of epigenetic domain screening utilizing the protein heterodimer system: *1:1'*. Different epigenetic effector domains fused to *1'* can be co-delivered and screened for activity at scale with a given keyhole-targeted DNA binding domain fused to the heterodimer partner, *1'*. (c) Genes from which candidate repressor domains were selected for screening. (d) The DNA binding domain of the TIM3 repressor TM18 was selected to screen additional functional domains. TM18-DBD was fused to heterodimer *1*, and a library of domains was fused to heterodimer *1'*. (e,f) Both constructs were transiently expressed in primary human T cells by RNA electroporation, and fraction of cells with TIM3 repressed (%TIM3 negative cells in TM18-treated cells relative to no RNA control) was evaluated periodically for 26 days by cell surface antibody staining and flow cytometry. Cells with greater fluorescence intensity than unstained control were considered TIM3+. (e) Domains containing KRAB showed more durable repression, or relatively slow kinetics of decay, for several different KRAB domains show on the left with conceptual diagram (right). (f) Domains from methyl-DNA binding proteins (see supplemental table S2) showed less durable repression, or relatively fast kinetics of decay (left), with conceptual diagram (right).